This is a non-peer-reviewed pre-print submitted to EarthArxiv

Use of Low Impact Development Systems to Enhance Recharge using Stormwater in a Heavily Groundwater-Depleted Region of the Gulf Coast Aquifer

Saheli Majumdar, Ph.D.[1*] and Gretchen R. Miller, Ph.D., P.E., P.G.[2]

[1]Zachry Department of Civil and Environmental Engineering,

Texas A&M University, 3136 TAMU, College Station, Texas 77843, USA.

[2]Texas Groundwater Lead, LRE Water, Round Rock, Texas 78681, USA.

[*]Corresponding author: Saheli Majumdar, majumdarsaheli07@gmail.com

ABSTRACT

Water resources in the Houston Metropolitan Area, otherwise known as Greater Houston, have been under enormous stress for decades due to an increase in population and uncertain climate conditions. Rapid urbanization has also increased impervious cover, leading to excess stormwater runoff. Implementing managed aquifer recharge (MAR) through the use of low impact development (LID) strategies can augment stormwater infiltration and help replenish groundwater resources in the region. However, research on the effects of LID practices on groundwater quantity and quality in the Greater Houston metropolitan area is limited. The main objective of this study was to evaluate and compare the impact of two LID systems and the native soil on groundwater recharge and chemistry. Three test cells representing native soil, soil amendment, and trench aggregates were constructed in a detention basin in a Houston suburb and their performance was evaluated over a two-year period. We found that trench aggregates recorded the highest mean cumulative infiltration over the monitoring period, 1.5 times that of

the soil amendment and 1.6 times that of the native soil. When the test cells were completely inundated, native soil registered a drainage of 773 mm which was 13 times that of trenches and 20 times that of soil amendment. The results from the infiltration data were supported by the groundwater elevation data. The groundwater quality was not highly affected during this study except for its salinity content. The findings suggest that retrofitting detention basins with LID systems helped enhance recharge over the long term. Native soil also facilitated significant infiltration when the detention basin was completely inundated for a prolonged period by modifying its outfall structure. The results from this study can help engineers better design existing stormwater detention basins to augment groundwater resources.

AUTHOR KEYWORDS: Low Impact Development; Managed Aquifer Recharge; Stormwater infiltration; Soil Amendment; Trench Aggregates.

INTRODUCTION

To sustain the economic and population growth of the Houston Metropolitan Area, groundwater from the Gulf Coast aquifer system has been excessively used since the early 20th century (Ellis et al. 2023). Such an overdraft of groundwater has lowered its levels by more than 300 ft and has caused more than 9 ft of land-surface subsidence in the Houston Metropolitan Area by late 20th century (Ellis et al. 2023; Greuter and Petersen 2021; Texas Living Waters 2017). From 2016 to 2020, the maximum land subsidence rate in the region was registered at 3.26 cm/year (USGS 2023). On the other hand, rapid urbanization in Houston has also contributed to more stormwater runoff in streams (Muñoz et al. 2018). Additionally, Houston is at risk from intense flooding from hurricanes due to its geographical location, and global warming is expected to intensify these disastrous storm events, resulting in increased flooding (Associated Press 2017; Blackburn and Borski 2023). To reduce the impacts of urbanization and improve resilience to climate

change, many cities are implementing the approach of sustainable urban water management (Brown et al. 2009), also known as low impact development (LID) (Rentachintala et al. 2022). LID refers to the implementation of practices that mimic pre-developmental conditions (Chui and Trinh 2016; Eckart et al. 2017; EPA 2021). LID practices help to significantly lower the quantity of runoff (Wang et al. 2019; Zahmatkesh et al. 2015), enhance infiltration (Ahiablame et al. 2012; Zhao et al. 2023), and promote groundwater recharge (Bhaskar et al. 2018; Mooers et al. 2018). In developed areas, LID technologies can be used to retrofit existing hydrological infrastructure (Ahiablame et al. 2013; Brander et al. 2007; CVC 2010; Damodaram et al. 2010; Fiori and Volpi 2020; Hu et al. 2019).

LID has been successfully implemented across the world (Eckart et al. 2017; Liu et al. 2021) and its performance evaluated (Beganskas and Fisher 2017). Infiltration through green infrastructure in shallow groundwater environments has been adequately quantified and evaluated using on-site monitoring and numerical modeling (Ganot et al. 2017; Lopes Bezerra et al. 2022; Zhang and Chui 2019). Infiltration dynamics were monitored in an infiltration pond where desalinated seawater was used for managed aquifer recharge (MAR) in Israel. Groundwater levels rose by 17 m due to month-long continuous MAR, and the recharge was reasonably captured by a numerical model (Ganot et al. 2017). Masetti et al. (2016) monitored a 16-ha infiltration basin in Northern Italy and observed that the facility, in absence of topsoil clogging, could boost the recharge of the underlying unconfined and highly permeable aquifer by more than fifty times when compared to the natural state. Since monitoring is limited to short periods, numerical modeling can be used to assess the effectiveness of such practices on urban stormwater management and aquifer recharge for extended periods (Ackerman and Stein 2008; Mooers et al. 2018; Wild and Davis 2009). A modified Storm Water Management Model (SWMM) was developed by Zhang et al. (2018), where the groundwater module of MODFLOW was integrated with SWMM to

simulate the effects of LID techniques in a shallow groundwater environment. The study found that the model estimated the subsurface hydrological variables such as groundwater levels and infiltration rates correctly.

When adopted in shallow groundwater environments, LID infrastructure can present many challenges. Infiltration of stormwater runoff can cause groundwater mounding which can harm the basements of neighboring homes and other structures (Carleton 2010; Yihdego 2017; Zhang and Chui 2019). Carleton (2010) inferred that groundwater mounds decrease in height when there is an increase in soil permeability, aquifer thickness, or specific yield. Short separation distance between the bottom of the LID structure and a seasonal-high groundwater table can lower the infiltration due to a smaller hydraulic gradient, thereby affecting the performance of the LID (Bouwer 2002; Jackisch and Weiler 2017). When the groundwater table is shallow, the infiltrating runoff may not be properly filtered due to low hydraulic residence time and can thus impair the quality of the ambient groundwater (Voisin et al. 2018). Zhang and Chui (2017) suggest that site-specific investigations must be carried out to ascertain the viability of a LID technique prior to implementation.

Infiltration-based systems used to manage stormwater can significantly affect groundwater recharge (Bhaskar et al. 2018; Lu et al. 2021; Newcomer et al. 2014). Typical rates vary between 20–300 acre-feet/year (USEPA 2003), but it also poses the challenge of groundwater contamination (Eckart et al. 2017). Lebon et al., 2023 underscores the need to consider the existence of preferential flow paths and quality of infiltrating water as they can affect groundwater chemistry, potentially impacting groundwater quality (Darling 2016; McQuiggan et al. 2022). Stormwater runoff from urban areas carry heavy metals, nutrient loadings, and volatile organic compounds (de Lambert et al. 2021; McGrane 2015). Hence it is necessary to treat the water infiltrating into the basin to prevent groundwater pollution.

Given how LID can alleviate the effects of excessive groundwater extraction by way of stormwater infiltration, it can also be used as a tool to contribute to MAR in the Greater Houston Metropolitan Area. This approach is unique in that LID technology is not only adopted to reduce stormwater runoff but also ascertain its impact on groundwater quantity and quality whereas it has previously been employed in the region as a tool to primarily control floods. This paper presents the findings from a pilot study which investigates the impact of LID strategies on surface infiltration and groundwater recharge in a stormwater detention basin in Houston. The performance of two LID systems was investigated and compared with that of the native soil. These systems were monitored over a period of 2 years to examine their effects on subsurface hydrological indicators such as groundwater levels, soil moisture, and drainage rate. The objectives of this study were to determine (1) which LID system facilitated more recharge in the detention basin under existing weather conditions and how they compare to the recharge under native soil, (2) which LID system infiltrated more water into the subsurface when stormwater ponded in the detention basin and how native soil performed under such conditions, and (3) how the treatments–or lack thereof–impacted the ambient water quality.

MATERIALS AND METHODS

Study Area

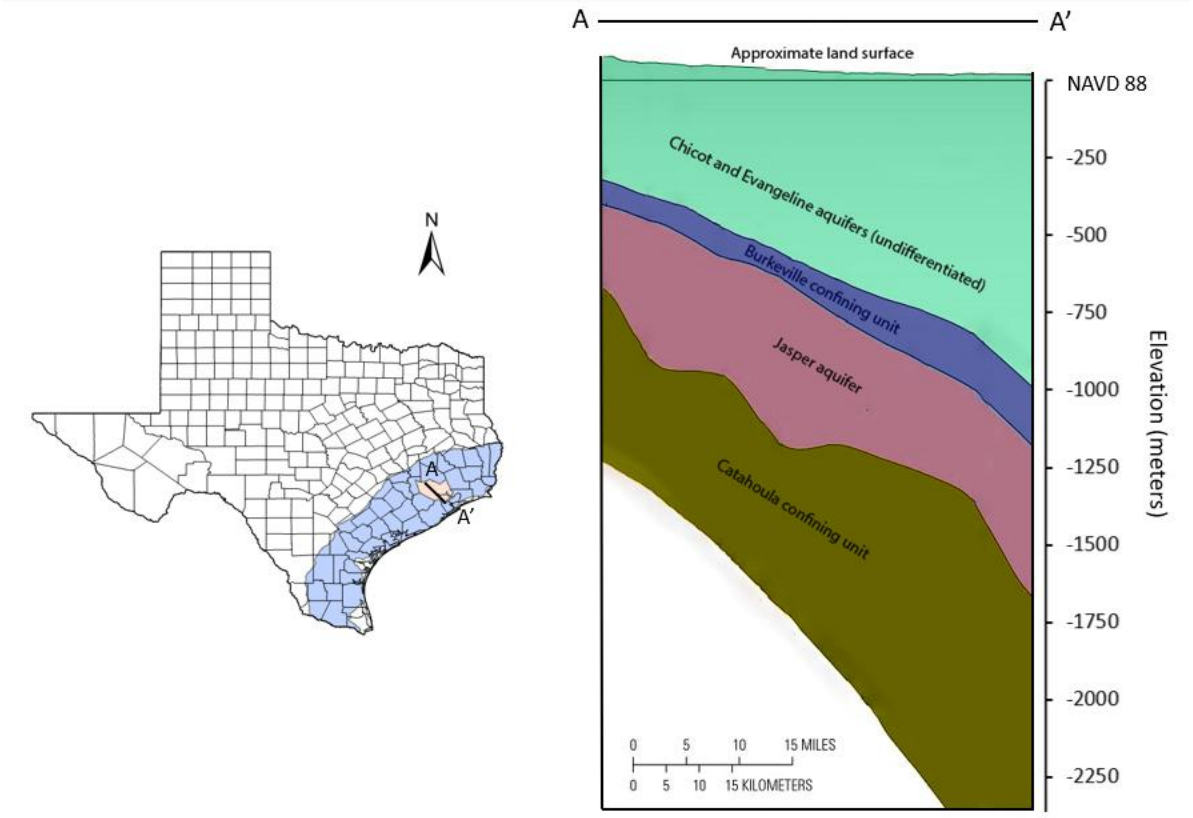

Figure 1: Cross-section showing the geologic units of Gulf Coast Aquifer in Harris County, Texas (modified from Ellis et al. 2023)

The study site was located within a detention basin in Tomball, Texas, USA, a suburb of Houston and part of Harris County (Figure 1). The detention basin was designed to occupy about 2 x 10^5 m^2 (50 acres) of land with a design depth of 3.96 m (13 ft) (Aviles Engineering Corp. 2003). Within the detention basin, three test cells of dimension 30.5 m x 30.5 m (100 ft x 100 ft) were marked out in the study area: one represented the native soil, and the other two test cells represented LID systems – a soil amendment and trench aggregates. The location of the test cells was chosen so that the center of each test cell was at approximately the same elevation. Note that the test cell representing native soil is also sometimes referred to as control test cell. The study site is hydraulically connected to Willow Creek. A tributary channel from Willow Creek begins flowing into the basin through a side overflow weir when the water level rises 0.61 m (2 ft)

above the average water level in the channel. The ground surface elevation of points located at the center of each test cell ranges from 45.65 - 46 m (150 - 151 ft), denoted by the grey colored bar in Figure 2, so the test cells will start to inundate when the water elevation in the channel exceeds this range. The water from the tributary channel spilled into the detention basin six times during the study period from January 2020 to December 2021 (Figure 2), but only completely inundated the test cells once. As seen in Figure 2, the streamflow from January 2020 to August 2020 is different from the standard trend which could be due to a fault in the sensor or an obstruction in the flow.

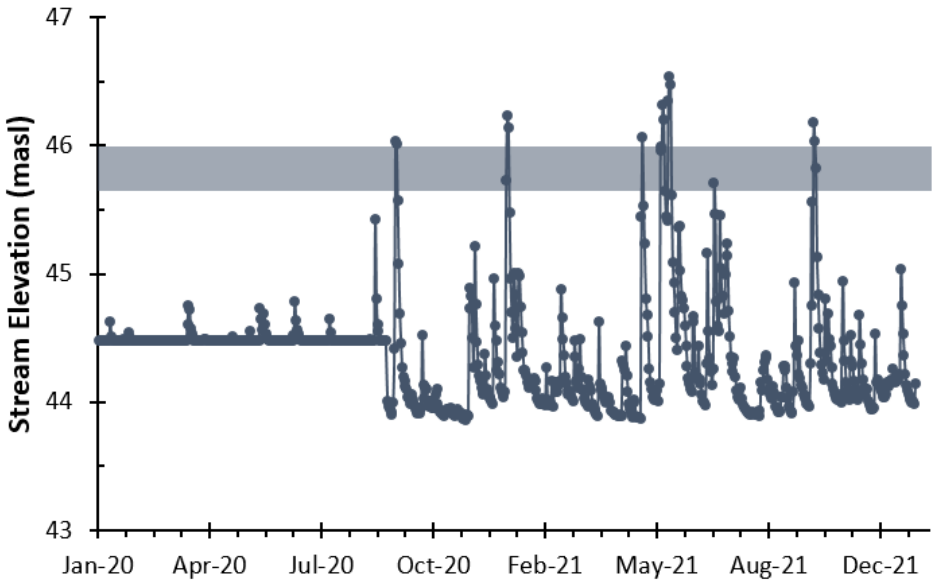

Figure 2: Stream elevation of Willow Creek recorded by Harris County Flood Warning System gauge during 2020-2021 (HCFCD, 2021). The horizontal, grey-colored bar represents the ground surface elevation of test cell centers.

Geology

The study site is underlain by the Gulf Coast Aquifer system which runs parallel to the Gulf of Mexico coastline, striking NE-SW and dipping toward the Gulf. The aquifer system is further classified into five hydrogeologic units listed from youngest (Holocene) to oldest (Miocene)

deposits: (i) Chicot aquifer (ii) Evangeline aquifer (iii) Burkeville confining unit (iv) Jasper aquifer (v) Catahoula sandstone, out of which the Chicot aquifer is the primary water bearing formation immediately beneath the test site. The Chicot and other hydrogeologic units of the Gulf Coast Aquifer system are unconfined inland where they are exposed at the earth's surface. The aquifer system becomes confined as its depth increases downdip. The outcrop region facilitates recharge into the confined aquifer system. The Chicot aquifer is composed of sediments that are lateral discontinuous beds of sand, silt, clay, and gravel deposited in layers (Baker 1979; Ellis et al. 2023; Kasmarek and Robinson 2004). The Chicot aquifer has a maximum thickness of 244 m (800 ft) in Harris County (Kasmarek and Robinson 2004). The transmissivity of the Chicot aquifer ranges from 914 to 7620 m^2/d (3000 to 25,000 ft^2/d), as was determined from aquifer-test data by Meyer and Carr (1979). This high transmissivity could potentially enable significant infiltration of water in the Chicot.

In addition, there are perched water tables in the Gulf Coast Aquifer System due to the presence of clay lenses within the aquifers; these restrict the downward movement of water to the regional water table (Chowdhury and Turco 2006). The study site has higher transmissivity as compared to other areas in Chicot aquifer (Smith et al. 2017), probably owing to the presence of Lissie formation near the surface of north-central Harris County. Although the Lissie formation is generally composed of unconsolidated sand, silt and clay, higher hydraulic conductivity near the ground surface suggests that the study region has more sand and silt and less clay, which would facilitate drainage of water.

Field and Laboratory Geotechnical Investigation

The detention basin was originally designed using shallow soil borings drilled to a depth of 5 m and 8 m, a sizable fraction of these materials was excavated during construction of the basins; it is typical to remove 4.6 – 7.6 m (15 – 25 ft) of overburden to allow for storage of stormwater in

166 case of a flood event. For purposes of this research study, the subsurface of the site was further
167 explored using geotechnical investigation, which enabled us to determine soil properties such as
168 particle size distribution, infiltration rate, and soil hydraulic parameters. Seven piezometers were
169 installed in the site to monitor groundwater levels: three of them were installed inside the basin
170 (at the center of each test cell) while the remaining four were installed on the raised platform of
171 land around the basin. Additionally, in order to determine the texture and infiltration rate of the
172 native soil, 8 holes with a depth of 0.61 m (2 ft) were dug in each of the three test cells, resulting
173 in a total of 24 test holes. The holes were dug at relatively similar locations within each test cell;
174 four of them were located near the corners and the other four were based near the center. Soil
175 samples collected from the middle of the test hole profiles were used to determine their grain-
176 size distribution. To determine the particle-size distribution of coarse-grained soils, we
177 performed sieve analysis according to the ASTM standard D6913/D6913M – 17 (ASTM D6913-
178 04 2017). Hydrometer analysis (ASTM D7928 2017) determined the particle-size distribution of
179 fine-grained soils smaller than 0.075 mm. The results from soil textural analysis showed that
180 sandy loam was the dominant soil type in the area. The average sand, silt and clay fractions were
181 52%, 41% and 7% respectively and the shear strength was estimated to be 2×10^5 N/m^2. ASTM
182 standard D3385 – 18 (ASTM D3385-18 2018) was used to determine the infiltration rate using
183 Double-Ring Infiltrometer and the average infiltration rate was established to be 0.21 m/day.

184 **Design of LID Systems Used in the Study**

185 ***Soil Amendment***

186 Soil amendment is soil mixed with other materials to increase its porosity and enhance its
187 properties such as infiltration, water retention, and permeability (DEP 2006; MPCA 2013). The
188 existing top (0.46 m or 18 in thick) soil in test cell-2 was replaced with amended soil (Figure 3a).

The test site was then seeded and mulched with Bermuda turf grass. The soil amendment was prepared by mixing the native soil with masonry sand and plant-based compost material.

Trench Aggregates

Trench aggregates are shallow excavated pits backfilled with coarse aggregates (no fines). Trench excavations were 0.91 m (3 ft) deep and 0.61 m (2 ft) wide with 1.83 m (6 ft) spacing between their centers in test cell-3. We discarded the excavated soil. An 8-ounce non-woven fabric lining was provided on the sides of trenches to prevent migration of material into the aggregate voids. The top 0.15 m (6 in) of the trenches were filled with ASTM Grade 5-7 while the remaining part of the trenches were filled with 0.05 m (2 in) to 0.1 m (4 in) crushed recycled concrete (Figure 3b). The disturbed areas of the test site were then seeded with Bermuda turf grass.

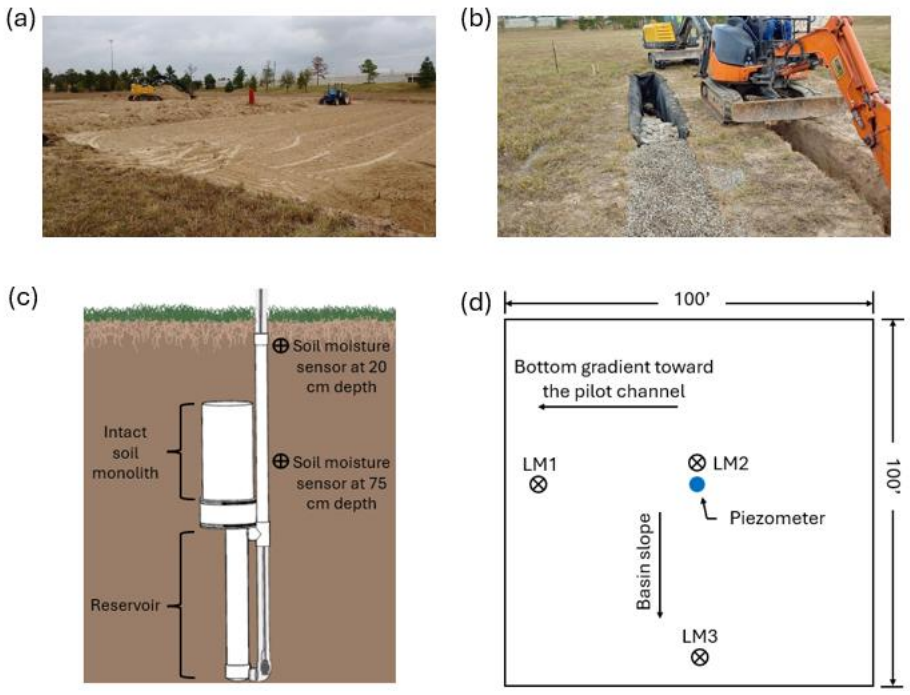

Figure 3: (a) Excavation of plot and mixing of native soil with amendment materials, (b) Trenches excavated and backfilled with rock gravel and recycled concrete aggregates, (c)

Schematic diagram of the lysimeter showing soil moisture sensor locations (modified from G3 Drain Gauge, METER Group, 2018), (d) Schematic diagram of the location of piezometer and lysimeters in control test cell

Smart-Pond Device at Basin Outlet

When the detention basin was originally constructed, a concrete junction box was installed at the outlet of the basin to facilitate longer holding times of stormwater and, in turn, increase the infiltration volume. The outfall structure allows for the basin fill when surface runoff occurs in Willow Creek. A check valve was also installed in the existing 24-inch outlet pipe to prevent the backflow of water into Willow Creek. An 8-inch orifice was used as an alternative to reduce the outlet flow rate to 10%. When the water level in the basin rises above 46.63 m (153 ft) during large storm events, an overflow inlet grate installed in the outfall structure allows the basin to function as originally designed. In this study, a device called 'Smart Pond', manufactured and distributed by Construction EcoServices, was also installed along with the outfall structure to discharge the stored water within 72 hours from the peak time of a rainfall event, as stipulated by Harris County Public Infrastructure Department Architecture & Engineering Division (HCPID-AED) and Harris County Flood Control District (HCFCD) Storm Water Management Programs. (HCFCD and HCPID-AED 2011). smartPOND® enables automatic measurement and release of stormwater to match regulatory guidelines using a web-based application (Construction EcoServices 2019). It comprises an automated rotating skimmer that rotates 90 degrees to open and close a rotary weir connected to an outfall pipe.

Subsurface Data Collection

After the LID systems were constructed in test cells- 2 and 3 (with test cell-1 being the native soil), monitoring equipment was installed. An ATMOS 41 weather station (ATMOS 41, METER

Group, 2018) was installed in the detention basin to measure weather variables such as air temperature, relative humidity, vapor pressure, barometric pressure, wind speed, gust and direction, solar radiation, precipitation, lightning strike counter and distance. A CTD-10 conductivity temperature depth sensor (CTD-10, METER Group, 2018) was installed in the piezometers located in the test cells. This sensor was used to continuously measure the groundwater depth, electrical conductivity, and temperature of the water. Drainage rates below the root zone were measured by a G3 drain gauge lysimeter (G3 Drain Gauge, METER Group, 2018). The lysimeter measures drainage rates by collecting water from an intact soil monolith. After a pre-set amount of water is collected in the lysimeter's reservoir (Figure 3c), it automatically triggers an attached peristaltic pump which then pumps out the water. The lysimeter also helps to determine the temperature and electrical conductivity of the water accumulated in its reservoir. Three lysimeters were set up in each of the test cells: one near the center of the plot and the remaining two near the center of two consecutive plot edges to capture the drainage rate along the basin slope and bottom gradient toward the pilot channel (Figure 3d). A pilot channel is a shallow channel that keeps water from standing still on the basin floor and directs stormwater to the outlet of the basin. For convenience, the lysimeters in the control plot are referred to as LM1, LM2 and LM3; the lysimeters in soil amendment plot are referred to as LM4, LM5 and LM6; the lysimeters in trench aggregates plot are referred to as LM7, LM8 and LM9. The letters B, C, G used in Figure 6b indicate the location of lysimeters in the test cells: B for basin slope, C for center, G for bottom gradient toward the pilot channel. To measure volumetric water content, temperature, and bulk electrical conductivity within the soil matrix, six TEROS 12 sensors (TEROS 11/12, METER Group, 2018) were used in each test cell. Two of these sensors were installed at a depth of 20 cm and 75 cm in the soil above every lysimeter soil monolith (Figure 3c). The sensors were then attached to a data logger which collects all the data and transmits them to an online database via the cellular network. All the data is collected at an

interval of 5 minutes. The groundwater level in all the piezometers was manually measured almost every month to calibrate the data obtained from the sensors. Groundwater was also sampled quarterly from the piezometers using the low-flow method (Puls and Barcelona 1996) to determine the impact of recharge on the quality of the ambient groundwater.

RESULTS AND DISCUSSIONS

Trend of Precipitation During the Monitoring Period

Harris County typically experiences hurricanes from June 1 to November 30. These hurricanes form due to warm ocean waters in the Gulf of Mexico. However, Harris County was either abnormally dry or in moderate to severe drought conditions for most of the monitoring period (NIDIS 2024). According to the US drought monitor, Harris County was in moderate to severe drought condition from mid-January to May of 2020 (Figure 4). Abnormally dry and moderate drought conditions again prevailed from November to December 2020. The year 2021 was comparatively wet though it had a few spells of drought. From March to May 2021, the entire county was abnormally dry, while a maximum of 40 percent of the county area was under moderate drought conditions during the same period; December 2021 was again abnormally dry (Figure 4). There was not a single storm event in 2020 that was able to completely inundate the detention basin. Tropical Storm Beta, which made landfall on September 21, 2020, on the southeastern coast of Texas, marked the onset of hurricane season and brought about 127 mm (5 in) of rainfall in the study area (Figure 5). The test cells were partly submerged in water due to this storm event. Precipitation events that led to partial submergence of test cells in water are henceforth referred to as partial inundation events. There was no significant rainfall event for the rest of 2020. As a result, the study was extended for another year to support our research with

multiple data points, the data points being inundation events. Three more partial inundation events occurred in 2021 along with one event where the detention basin was completely inundated (Table 1).

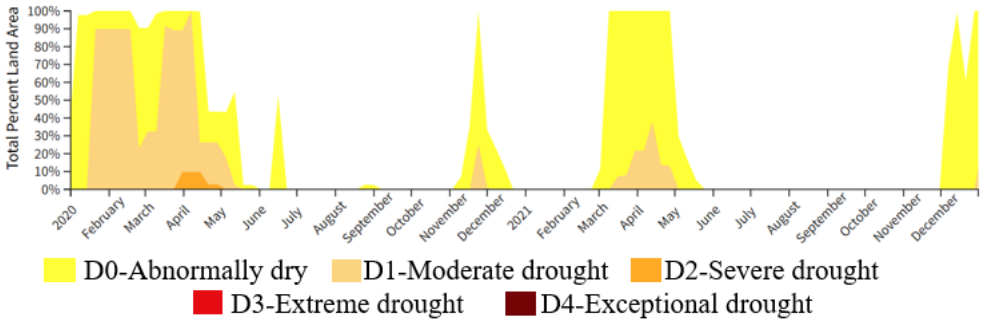

Figure 4: Abnormally dry conditions or moderate to severe drought conditions prevailed in Harris County for the bulk of the monitoring period (NIDIS 2024).

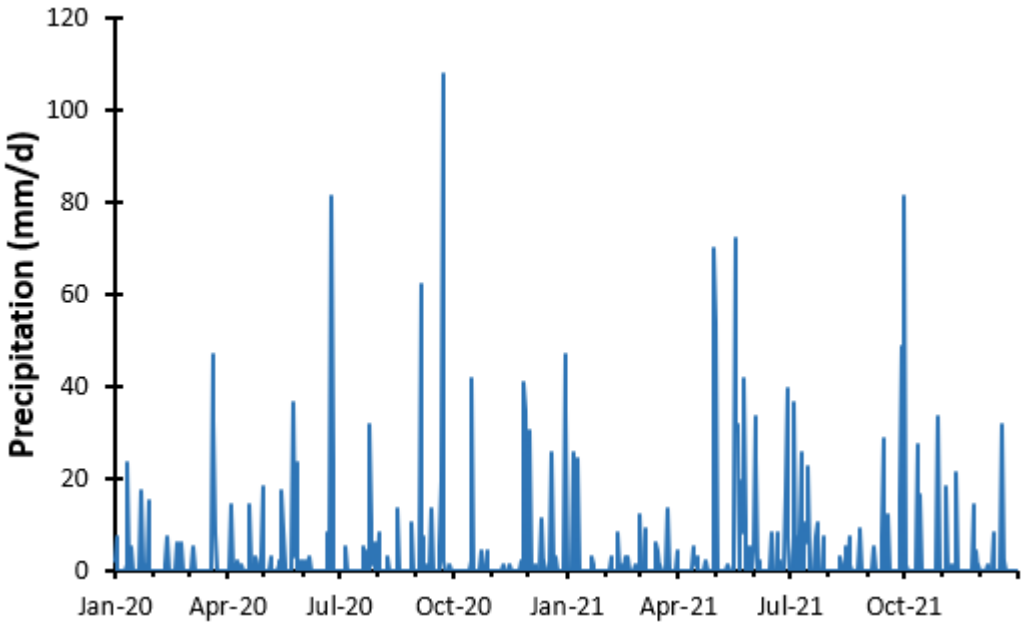

Figure 5: Daily precipitation varied in intensity over the span of the monitoring period with a maximum of 107.7 mm rainfall recorded in September 2020.

Types of events	Duration of events	Rainfall totals (mm)
Partial inundation	September 20-23, 2020	134
	December 30-31, 2020	81
	April 30 – May 1, 2021	124
	September 29 – October 1, 2021	130
Complete inundation	May 16 – May 29, 2021	234

Table 1: The study area witnessed five major storm events from 2020 to 2021.

Behavior of LID Systems and Native Soil During the Monitoring Period

Total Infiltration was Highest in Trench Aggregates

The drain gauge lysimeters measured deep drainage underneath the root zone in the three test cells. Average cumulative infiltration was used to compare the infiltration potential of the three test cells, and it was obtained by averaging the total infiltration accumulated throughout the monitoring period across the three lysimeters. The trench aggregates test cell recorded the

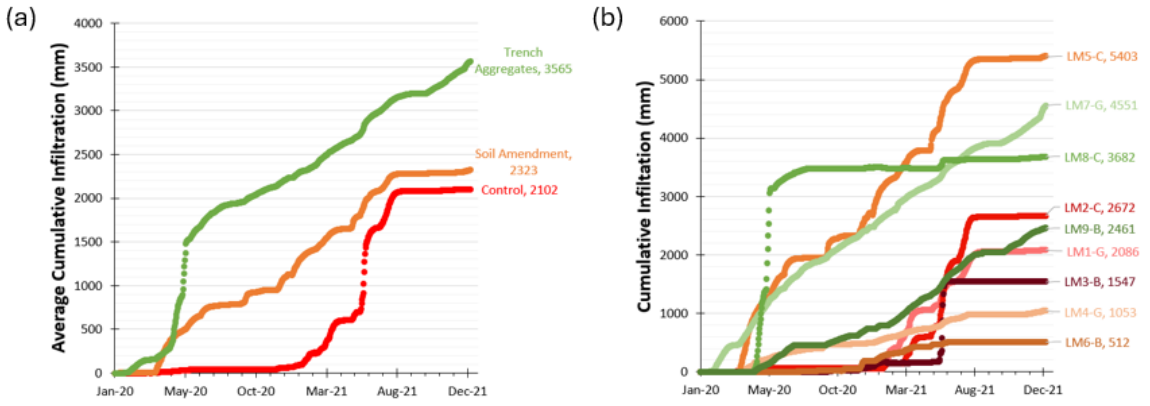

Figure 6: (a) Cumulative infiltration is highest in trench aggregates on average, (b) Cumulative infiltration is also markedly different for the three lysimeters in each test cell.

highest average cumulative infiltration (Figure 6a), which was 3.36 m, followed by the soil amendment test cell (2.29 m) and control test cell (2.09 m). The trench aggregates test cell also registered infiltration earlier in the monitoring period (January 2020) than the other two test cells. The average soil moisture content at the time the infiltration began was 0.2 and 0.22 m^3/m^3 at 20 cm and 75 cm depth respectively (Figure 9). It is important to note that the soil moisture sensors along with the lysimeters in the trench aggregates test cell were installed in the native soil between the trench excavations, although we used one sensor to measure the water content within the aggregates directly. We preferred this arrangement because it helped us understand the impact of trench aggregates on the hydraulic conditions of native soil. The aggregates in the trenches had large pore spaces and did not retain water for long. High vertical and lateral suction gradients further down the soil eventually led to significant drainage in the trench aggregates test cell earlier in the monitoring period. The next test cell to register infiltration was soil amendment. It began to record drainage from March 2020 (Figure 6a). When infiltration commenced, the average soil moisture content at 20 cm and 75 cm depth in the soil amendment test cell was 0.22 and 0.27 m^3/m^3 respectively (Figure 8). At the given moisture content, it was likely that the soil matric potential had reduced considerably, hence the water was not held very strongly by the soil matrix, enabling it to drain freely. The control test cell came in a close third. Though the rainfall events in the first year of the monitoring period had almost no effect on drainage in the native soil, we started to record significant drainage since the start of the second year (2021) of the monitoring period (Figure 6a). Negligible to low infiltration was observed in native soil in 2020, which can be attributed to the presence of hysteresis. Since the native soil was medium-textured sandy loam, soil water redistribution was slow, resulting in slower internal drainage (Figure 7). A combination of high matric suction gradient and higher water content in

general made the soil pores conducting and led to a surge in infiltration towards the beginning of 2021.

The soil amendment test cell registered a steady infiltration throughout the monitoring period. The organic matter in soil amendment likely helped in soil aggregation, which resulted in an increase in porosity and infiltration. The trench aggregates test cell exhibited significantly higher infiltration across the monitoring period. Large pore spaces in aggregates facilitated fast drainage of water leading to high vertical and lateral suction gradients in the adjacent native soil, causing rapid soil water redistribution. As a result, the soil water content increased, making the pores conductive. Native soil recorded a substantial amount of infiltration from early 2021 until August 2021 (Figure 6a). A steep rise in infiltration was observed in May 2021 when the stormwater detention pond was under 1.75 ft of ponding water depth; the factors contributing to this situation are described in detail in the *Performance under Inundation Event* section.

The slope of cumulative infiltration over time for soil amendment and control test cells approached zero towards the end of the monitoring period, implying that the infiltration rates for both the test cells reached a constant asymptotically (Figures 6a and 6b). This rate is termed as the final infiltration capacity (Hillel 1980). The infiltration rates for soil amendment and control test cells over the last five months attained an average value of 0.19 and 0.21 mm/d respectively, hence these are the corresponding final infiltration rate capacities. The reduction in infiltration capacities could have been caused by the progressive degradation of soil structure, swelling of clay and blocking of pores by foreign particles.

LID Systems Experienced Higher Infiltrability as Demonstrated by Soil Moisture Graphs

Figures 7, 8 and 9 present the variation of soil moisture and drainage with time for all three test cells. The soil moisture content and its corresponding fluctuation over time had significant implications for infiltration, which is explained in the following paragraphs.

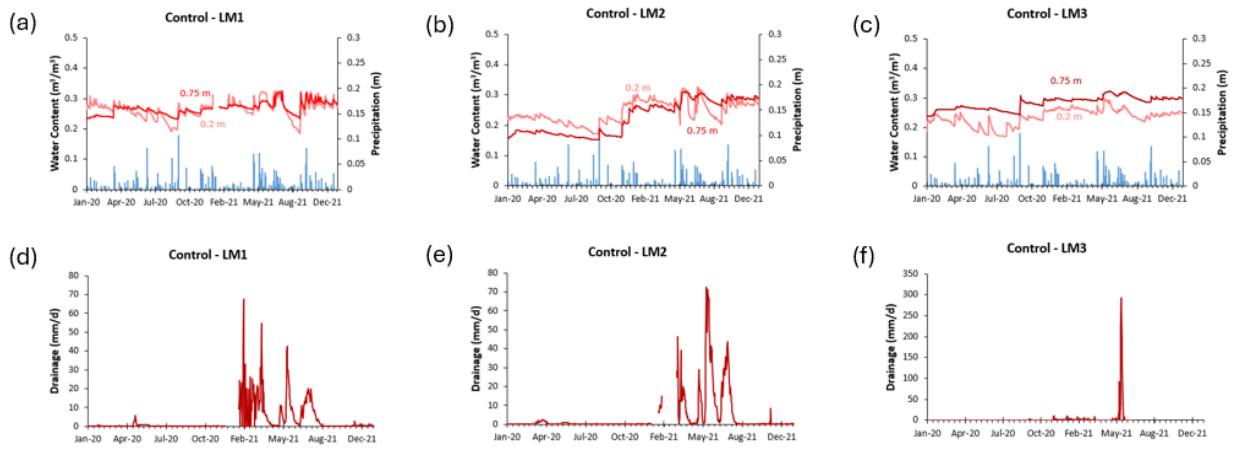

Figure 7: Soil water content for control test cell with native soil was characterized by pronounced hysteresis in the first half of the monitoring period leading to negligible drainage. Significant drainage was observed in the later half of the monitoring period.

For LM1, which is located along the bottom gradient toward the pilot channel of the test cell, hysteresis caused a slow water redistribution. The moisture content at 75 cm depth increased after an 87 mm storm event in mid-March 2020 (Figure 7a) implying there was internal drainage but not enough to register infiltration underneath the root zone. An appreciable matric suction gradient of 12.6% initiated internal drainage that resulted in an infiltration rate of 25.2 mm/d following a 6 mm rainfall event in February 2021 (Figure 7d). The matric suction gradient was substantial for the subsequent months which likely saturated the pores enough to make them conductive. As a result, a total drainage of around 2.1 m was recorded. In the case of LM2, located at the center of the test cell, the matric suction gradient ranged from 12% to 45%, yet no significant infiltration was registered in 2020. The volumetric water content was very low, leading to high matric suction forces, hence the soil matrix held on to the water tightly resulting in zero to negligible infiltration. A precipitation event of 75 mm spread across two days in November 2020 caused a matric suction gradient of 43% increasing the soil moisture at 75 cm depth by approximately 17% to 0.2 m^3/m^3, hence causing internal drainage (Figure 7b). Subsequent storm events also facilitated internal drainage and raised the soil moisture content at

the same depth to around 0.26 m^3/m^3. Internal drainage possibly made the pores saturated enough to be conductive. Additionally, progressive saturation likely reduced tortuosity and hence infiltration was registered from January 2021 (Figure 7e). On the other hand, LM3, located along the basin slope of the test cell, hardly recorded infiltration throughout the monitoring period except under inundation (Figure 7f). It can be attributed to the heterogeneity of the native soil and that clay content was higher locally which resulted in higher matric suction forces and negligible drainage (Figures 7c and 7f). Interestingly, there was an appreciable difference in the cumulative infiltration observed for the different lysimeters (Figure 6b). Soil heterogeneity plausibly resulted in non-uniform hydraulic conductivity leading to varying head gradients in different regions of the test cell and thus causing distinct trends in drainage.

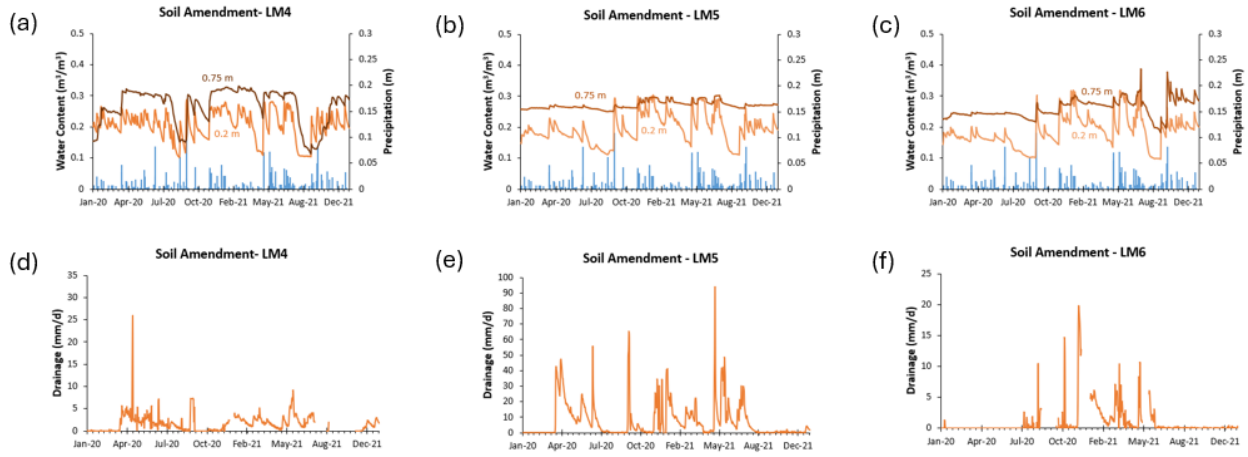

Figure 8: Well graded soil in soil amendment test cell facilitated faster soil water redistribution leading to significant drainage over the span of the monitoring period.

The soil amendment was very sensitive to precipitation; the soil water content at 20 cm depth peaked immediately after a storm event and the rise was twice as high when compared to the control test cell throughout the entire monitoring period (Figures 8a, 8b and 8c). The higher amplitude of water content near the surface suggests that soil amendment had higher infiltrability. The highest amplitude recorded was when the water content at 20 cm depth (for LM6) jumped from 0.1 m^3/m^3 to 0.3 m^3/m^3, logging a 200% rise, during Tropical Storm Beta

(Figure 8c). Internal drainage for LM5 and LM6 was fast (Figures 8b and 8c) thus the soil pores further underground were easily saturated and consequently turned conductive. Hence, substantial infiltration was recorded over the course of the monitoring period (Figures 8e and 8f). Rapid internal drainage for LM4 caused a sharp rise in soil moisture content at 75 cm depth in January 2020 (Figure 8a). Subsequent storm events kept the moisture content elevated at approximately 0.31 m^3/m^3 for most of the monitoring period (Figure 8a), and the saturated pores facilitated drainage (Figure 8d). When the cumulative drainage for different lysimeters in the soil amendment test cell was examined, LM5 emerged to have a considerably higher drainage than both LM4 and LM6 combined (Figure 6b). Located at the center of the test cell, LM5 benefitted from the higher infiltrability of soil amendment and consequently, fast soil water redistribution. LM4 and LM6 recorded low overall drainage as they were located near the edges of the test cell, low infiltrability of the native soil was anticipated to have caused lower suction gradients and in turn, caused lower drainage.

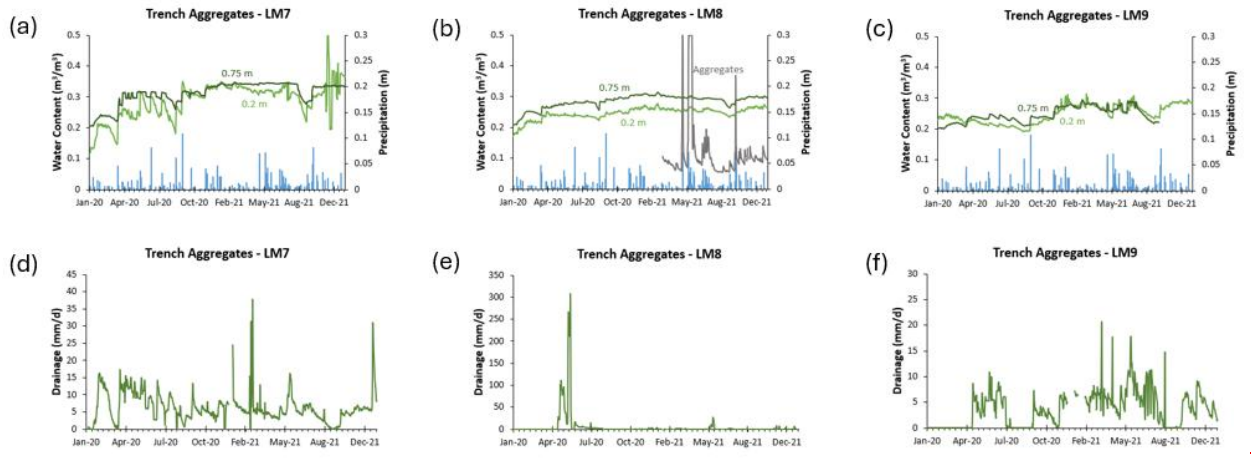

Figure 9: Low storage capacity of aggregates resulted in fast drainage in top soil. Rapid soil water redistribution helped make the trench aggregates test cell the first to register drainage.

The trench aggregates test cell was also sensitive to precipitation, as evidenced from the soil moisture content at 20 cm depth for LM7 and LM9 (Figures 9a and 9c). The impact of trench

aggregates on native soil was evident in that there was steep rise and fall of soil moisture content at shallower soil depths for LM7, suggesting that the trench aggregates test cell had a high infiltrability and therefore recorded significant drainage (Figure 9d). The depth-to-groundwater was low for trench aggregates, and hence, the soil pores located slightly deeper from the surface neared saturation. As a result of low vertical gradient, it took longer for the soil to drain, thus giving rise to a step-like trend. The water content at 75 cm depth was sustained at 0.34 m^3/m^3 for a major part of 2021 (including the complete inundation event) suggesting that it had reached the saturation level (Figure 9a). For LM9, no infiltration was recorded in the first three months of 2020 (Figure 9f). Vertical and lateral suction gradients helped raise the soil moisture content at 75 cm depth from 0.21 m^3/m^3 to 0.24 m^3/m^3 after an 87 mm storm event in mid-March 2020 (Figure 9c). Subsequent storm events likely raised the soil moisture content of the pores underneath making them conductive and as a result, infiltration was registered in April 2020 (Figure 9f). Multiple rainfall events increased the water content at both the near-surface and deeper soil thereby resulting in a significant infiltration for LM9. For LM8, any rise and fall in water content at 20 cm depth was almost immediately followed by a corresponding leap and plunge in water content at 75 cm depth, suggesting a rapid redistribution of soil water (Figure 9b). Similar to LM9, LM8 started recording infiltration in April 2020 which reached a peak value of 301 mm in May 2020 (Figure 9e). Thereafter, the infiltration rate reduced to an average constant rate of 0.5 mm over the next couple of weeks which could have been caused due to swelling of clay in the native soil. The aggregates logged a water content of 0.5 m^3/m^3 during storm events that partially or completely inundated the test cells implying that their large pores helped capture more water (Figure 9b). Additionally, there was a sharp decrease in water content right after the event suggesting that the aggregates had low storage capacity and did not retain water for long. Furthermore, there was a marked difference in the overall drainage for all the lysimeters in the trench aggregates test cell which can be ascribed to their respective locations.

LM8, owing to its central location, peaked very fast while the rise in drainage for LM7 and LM9 was gradual (Figure 6b) as they were situated closer to the edges of the test cell and were most likely influenced by the low infiltrability of the surrounding native soil.

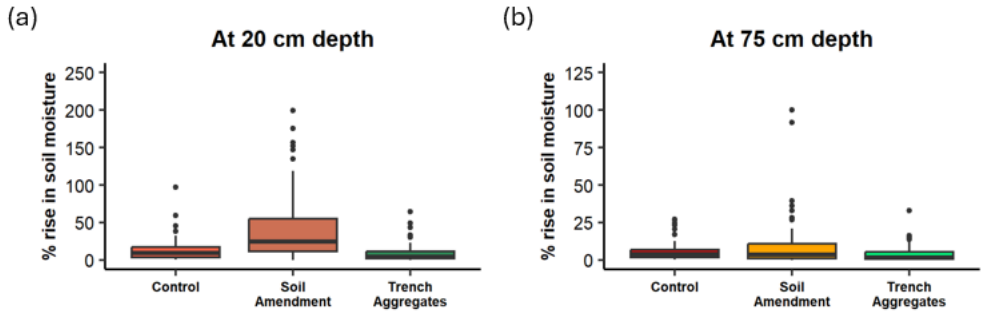

Figure 10: Variability in the increase in soil moisture at a depth of a) 20 cm b) 75 cm

A unique analysis was performed to compare the percentage rise in soil moisture after significant storm events for each test cell at both 20 cm and 75 cm soil depths. Any events that brought 20 mm of rainfall or more were considered. The maximum soil water content corresponding to that event was identified and compared with the soil moisture condition that existed prior to the storm event to calculate the percentage rise in soil water content. Soil amendment registered the highest average increase in soil moisture after a precipitation event in shallower depth (Figure 10a). The soil moisture content at a depth of 20 cm increased by a maximum of 200% in soil amendment after Tropical Storm Beta. This suggests that the amended soil had high infiltrability, reinforcing the conclusion drawn from the soil moisture graphs in Figure 8, and is favorable for shallow rooted vegetation (as was evident by the presence of highly dense local flora). The effect of storm events was lower as the soil profile depth increased (Figure 10b). The median value for increase in soil water content at 75 cm depth was roughly similar in all the test cells (within 2% - 4%) which was probably due to the presence of native soil at that depth (Figure 10b).

Trench Aggregates Kept the Groundwater Levels Elevated

443 The depth-to-groundwater was the lowest for trench aggregates, followed by soil amendment and
444 control test cells (Figure 11). The trench aggregates yielded the maximum amount of recharge
445 out of the given systems. While the groundwater levels in the control and soil amendment test
446 cells were comparable in February 2020, the groundwater level was higher by 1.2 m under the
447 trench aggregates during the same period, implying that trench aggregates registered higher
448 recharge since the start of the monitoring period. The colored dots in Figure 11 refer to the water
449 level measurements taken manually over the course of the monitoring period to calibrate the
450 measurements recorded by pressure transducers. Any surge in groundwater elevation was
451 observed immediately after infiltration was registered in the test cells. The groundwater decline
452 observed in the test cells after a considerable amount of time had passed after the infiltration
453 process suggested that the recharged groundwater moved vertically downward and laterally, thus
454 demonstrating the presence of a perched water table. This phenomenon along with negligible
455 infiltration caused the water table underneath the control plot to decline by approximately 4 m
456 from July 2020 to November 2020. It rose considerably by March 2021, which was
457 commensurate with the significant infiltration recorded in the native soil since the beginning of
458 2021. It is to be noted that there were some data gaps in the groundwater level measurement for
459 native soil owing to a malfunctioning pressure transducer; however, the groundwater level was
460 measured using a water level meter to monitor the groundwater level trend in the native soil
461 during that period. While the groundwater level under the trench aggregates was the highest out
462 of all the test cells for the entire period of record, the highest recharge was recorded in the
463 control test cell during the complete inundation event followed by the soil amendment and
464 finally the trench aggregates. Under complete inundation, the test cells experienced groundwater
465 mounding, causing the groundwater to rise above the ground elevation of the detention basin by
466 0.23 m in the native soil, 0.42 m in the soil amendment and 0.66 m in the trench aggregates.
467 Figure 11 shows the enormous impact of the complete inundation event on the native soil, which

led to a jump of 2.4 m in groundwater elevation in May 2021 within a span of 16 days. Finally, the groundwater level for all the test cells supports the evidence that the trench aggregates recorded the highest drainage (as measured by the lysimeters) and as a result, yielded the highest recharge. It is also important to note that while there was noise in the groundwater elevation dataset for trench aggregates, the groundwater level data was easily discerned and it was commensurate with the water level information gathered manually.

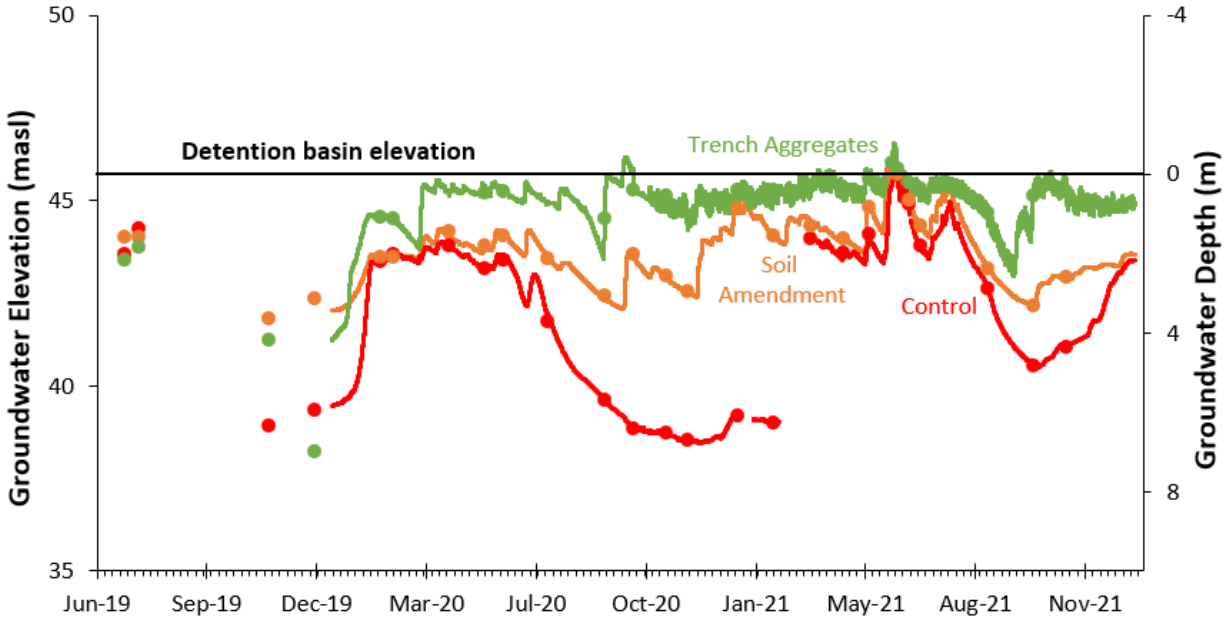

Figure 11: Trench aggregates consistently recorded the highest groundwater elevations, followed by soil amendment and control.

Performance under Inundation Event

A major storm event in the beginning of May 2021 inundated the test cells partially. This partial inundation event was followed by another storm event two weeks later which brought about 227 mm of rainfall over a span of 10 days, which again partially inundated the basin. The Smart Pond device was activated for 3 days, during which the weir connected to the outfall pipe was closed, contributing to the complete inundation of the study site. A maximum of 0.53 m (1.75 ft) of

water was accumulated in the basin during this period (Figure 12). Since there was a partial and complete inundation in the month of May, we discussed the tremendous impact it had on the infiltration rates of the test cells in this section.

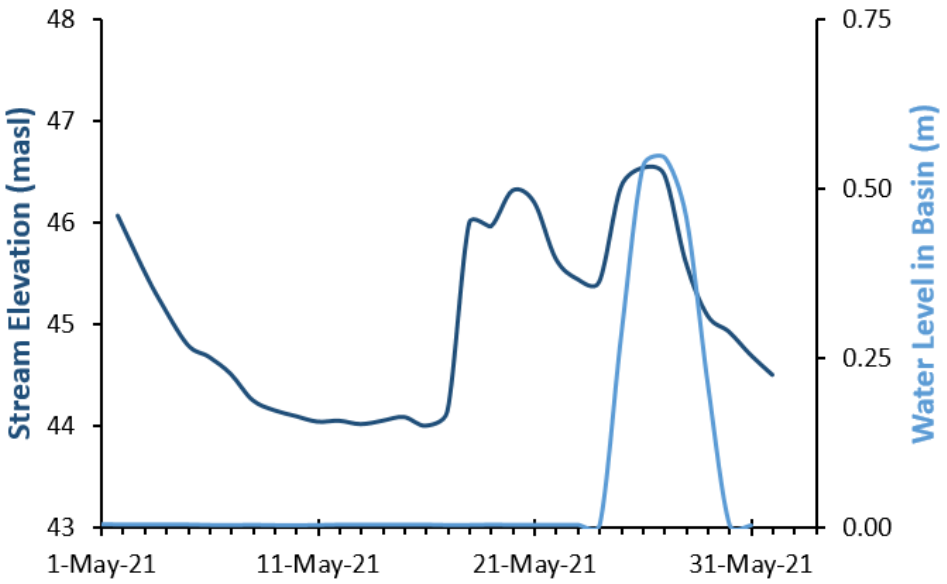

Figure 12: The detention basin was under a maximum ponding depth of 0.53 m on May 27, 2021.

During the inundation event, the control plot registered a maximum infiltration of 0.77 m, which was 20 times that of soil amendment and 13 times that of trench aggregates (Figure 13). The longer the basin was ponded with water, the greater the magnitude of infiltration in the control plot. The control test cell exhibited an exponential rise in cumulative infiltration from May 25 to May 31, 2021 (Figure 13). Infiltration for control was higher during the inundation event in May (a maximum rate of 0.29 m/d was observed) as the ponded water caused the pressure to be significantly higher than the atmospheric pressure, which caused a high potential gradient and moved the water down the soil at a rate higher than its infiltrability (Hillel 1980) which was a maximum of 0.03 m/d. This can be further substantiated by the soil moisture graphs (Figures 7,8, and 9): average volumetric water content at the center of control test cell increased by around 61 and 24 percent at 20 cm and 75 cm depths respectively under complete inundation, implying that

500 the soil pores in the native soil were close to saturation. The water phase became continuous
501 resulting in a higher conductivity and upsurge in infiltration. The average volumetric water
502 content for soil amendment test cell increased by around 52 and 8 percent at 20 cm and 75 cm
503 depths, respectively, while the average volumetric water content for trench aggregates test cell
504 grew by around 5 and 2 percent at 20 cm and 75 cm depths respectively. The low rise in
505 volumetric water content at 75 cm depth suggests that the soil deeper down in the soil
506 amendment and trench aggregates test cells was already saturated by the time the site was
507 completely inundated. Hence both the LID systems' infiltration rates were comparable with
508 those observed during the rest of the monitoring period. Longer detention time resulted in higher
509 ponding depth, thereby inducing an increase in hydraulic conductivity and infiltration rate in
510 native soil. Although longer detention times promote more recharge, it could potentially harm
511 the native plants or turf grass normally used to vegetate the bottom of the detention basins.
512 Hence it would be better to detain the water in the detention basin for no more than 5 days.

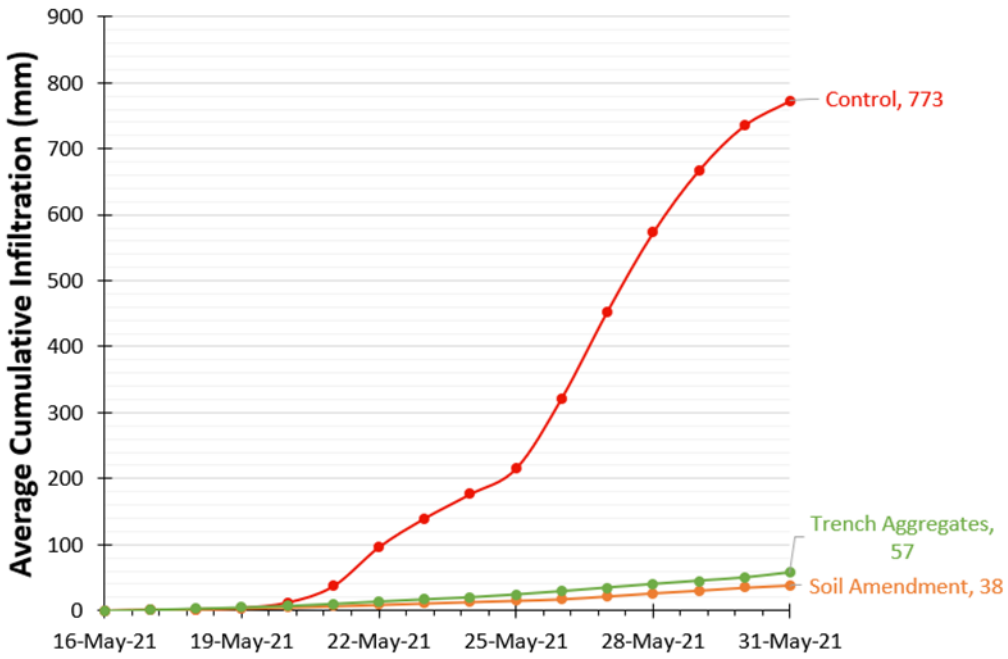

513

Figure 13: Control test cell recorded rapid growth in infiltration under longer detention times.

The phenomena behind the sudden jump in infiltration in the native soil can be also explained by Figure 14. Owing to hysteresis, the native soil experienced low infiltrability and slow soil water redistribution. As a result of low soil water content, the high matric suction forces led to low drainage. Multiple storm events over the course of the first year of the monitoring period increased the surface soil water content, leading to a high matric suction gradient and a rise in internal drainage. Consequently, conductivity increased and a rise in infiltration was registered. Figure 14 demonstrated that the infiltration rate in the control plot steadily increased from the September 2020 partial inundation event by 3.67 times and 15 times during successive partial inundation events. On the other hand, the soil amendment and trench aggregates recorded nearly consistent infiltration throughout the partial inundation events (Figure 14). The results from the complete inundation event proved that existing detention basins could also enhance groundwater recharge when longer detention times are allowed.

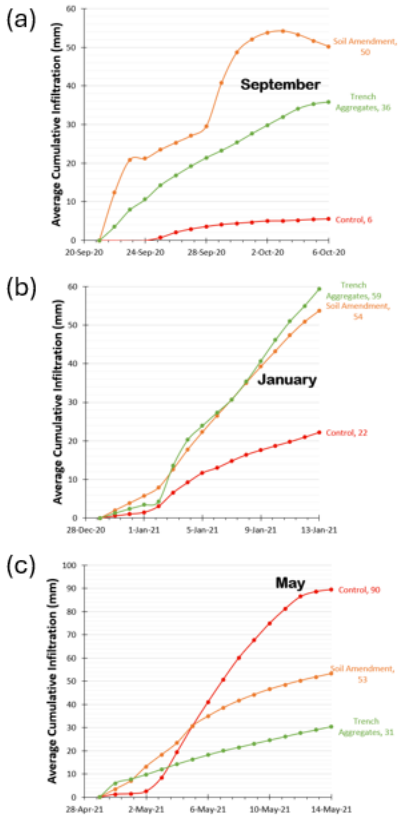

528

529 **Figure 14: Performance of the test cells in (a) September 2020 (b) January 2021 (c) May**

530 **2021 under various partial inundation events leading up to the complete inundation event**

531 **in late May.**

532 ***Assessment of Infiltration Potential of Test Cells under Varying Conditions***

	During the entire monitoring period from 2020-2021			
	Along the basin slope		Along the bottom gradient toward the pilot channel	
Test cells	Average cumulative infiltration (m)	Expected diurnal infiltration (m)	Average cumulative infiltration (m)	Expected diurnal infiltration (m)
Control	2.1096	0.0029	2.3792	0.0033
Soil amendment	2.9576	0.004	3.2279	0.0044
Trench aggregates	3.0714	0.0042	4.1165	0.0056

533

534

	During the May 2021 inundation event			
	Along the basin slope		Along the bottom gradient toward the pilot channel	
Test cells	Average cumulative infiltration (m)	Expected diurnal infiltration (m)	Average cumulative infiltration (m)	Expected diurnal infiltration (m)
Control	1.015	0.0634	0.4809	0.03
Soil amendment	0.019	0.0012	0.046	0.0029
Trench aggregates	0.0052	0.0003	0.081	0.005

Table 2: The daily infiltration is expected to be higher in native soil under complete inundation while LID systems are expected to record higher infiltration when the entire monitoring period is considered.

The infiltration potential for all the test cells across the span of the monitoring period was compared against that under complete inundation. Cumulative infiltration was averaged across two lysimeters along the basin slope and the bottom gradient toward the pilot channel in each of the test cells. Subsequently, we determined the expected diurnal infiltration for the whole monitoring period and May inundation event by dividing the average cumulative infiltration by the number of days encompassing that period i.e., 731 and 16 days respectively. The daily infiltration in native soil is expected to be 22 times higher along the basin slope and 9 times higher along the bottom gradient toward the pilot channel under complete inundation (Table 2). On the other hand, the LID systems are expected to register a maximum of 14 times higher daily infiltration along the basin slope and 1.5 times higher daily infiltration along the bottom gradient toward the pilot channel during the entire test period. Note that the diurnal infiltration anticipated in Table 2 may differ from the diurnal infiltration physically observed based on the depth of precipitation, stormwater ponding depth and antecedent soil moisture conditions. This postulation is corroborated by the fact that the performance of control cell was enhanced as it was primed by several storm events before the inundation event while all the test cells in the

study area underwent significant spells of drought over the span of the monitoring period thereby lowering the overall average drainage.

Impact on Water Quality

Groundwater was sampled quarterly from wells located inside the basin and on the berm, (wells on the berm are referred to as background wells), to keep a check on the quality of water being recharged into the system. Stormwater samples were also collected after 3 storm events that led to partial inundation of the basin. Except for salinity, the groundwater quality was not significantly affected. The total dissolved solids (TDS) concentration (an indicator of salinity) in the groundwater samples was elevated and it could have been caused by the infiltrating water that likely changed the redox state of chemical species thereby immobilizing the salts present in the sub-surface matrix. Among the test cells, trench aggregates leached the highest amount of salts into the groundwater (3680 ppm after the initial flush and 2370 ppm in the last sampling quarter) which was due to the recycled concrete aggregates used to backfill the trench aggregates (Figure 15a). The second highest TDS concentration was found in the control test cell, with a concentration of 2070 ppm registered in the last quarter. Groundwater sampled from control and trench aggregates test cells have TDS higher than Maximum Contaminant Level (MCL) (i.e., 1000 ppm), and hence cannot be distributed in public water systems without undergoing treatment according to USEPA. Notably, there was lower TDS in the background wells as compared to that of the control test cell because the detention basin got inundated more often therefore leaching more salts and affecting the ambient groundwater. Furthermore, the TDS present in stormwater was well below USEPA's secondary drinking water standard of 500 ppm, which reinforced that the salts flushed into the groundwater did not originate from the stormwater but from the subsurface soil deposits. The salinity in groundwater collected from the soil amendment was way below the MCL (ranging from 420 ppm to 862 ppm) making this

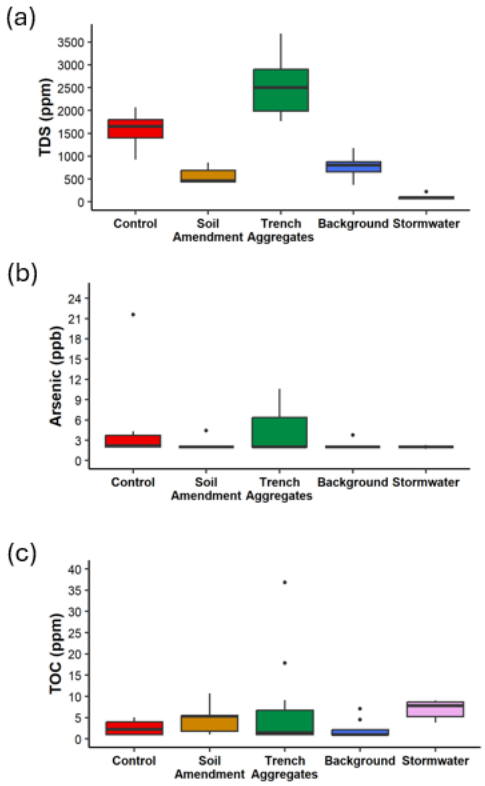

577

578 **Figure 15: (a) Soil amendment leached least amount of TDS. (b) Arsenic was largely**
579 **undetected and exceeded its MCL once in the groundwater sample from the control test**
580 **cell. (c) All groundwater samples had roughly similar TOC concentrations.**

581 LID system a desirable option when groundwater quality is of concern. Moreover, it would be
582 safe to conclude that the saline build-up leaching into the groundwater mostly emerged from the
583 topsoil, as the soil amendment differed from the other test cells in the top 0.46 m (18 in) soil
584 profile.

585 Groundwater samples were also tested for major ions, trace metals, and nutrients. Arsenic was
586 generally below the detection limit in all the groundwater samples except for once when it was
587 found to be above the permissible range (above 10 µg/l) in a control test cell lysimeter after the
588 initial flush (Figure 15b). In this case, the arsenic may have leached from the shallower
589 subsurface deposits and might have dissolved or been adsorbed by the subsurface medium before

590 the infiltrating water reached groundwater, as there were no traces of arsenic in groundwater
591 samples. While cadmium and mercury were found to be below the laboratory limits of detection,
592 copper, zinc and nitrate were below the MCL. Total Organic Carbon (TOC) is another water
593 quality parameter that is not harmful in itself but it can react with disinfectants present in water
594 to form disinfection byproducts. These disinfection byproducts, if present above a certain limit,
595 may prove to be harmful. Haloacetic acids and trihalomethanes pose increased risk of cancer if
596 present above 0.06 mg/l and 0.08 mg/l respectively (EPA 2021). The concentration of TOC
597 present in different samples did not vary much (all within 11 ppm except for a few outliers).
598 Since the detention basin is closer to a gas station, the water recharged from the basin has a
599 significant amount of TOC (Figure 15c). Groundwater and stormwater samples were also tested
600 for fecal contamination. A high count of E. coli (a maximum of 3 MPN per 100 ml) and total
601 coliform bacteria (ranging from 1 to more than 2420 MPN per 100 ml) was found in
602 groundwater samples, which was likely due to the increased infiltration of stormwater.
603 Disinfection, a very common procedure in water treatment plants, can reduce the number of
604 harmful microorganisms and help render the groundwater safe for potable purposes.

605

606 **CONCLUSIONS**

607 Rapid industrial and population growth in 20th century Houston led to an overreliance on
608 groundwater and subsequently caused lower groundwater levels and land subsidence. Moreover,
609 warmer ocean temperatures will bring about intense rainfall events and will likely lead to
610 increased flooding. To mitigate the consequences of groundwater overdraft and flooding, low
611 impact development practices can be adopted. To this end, the influence of LID systems such as

soil amendment and trench aggregates on groundwater recharge was monitored for two years and compared with that of the native soil.

The LID systems performed optimally with respect to subsurface hydrological variables such as groundwater levels, soil moisture, and drainage rate throughout the monitoring period. The native soil functioned well when the detention basin was ponded with stormwater for an extended period of time. Trench aggregates yielded the highest recharge and therefore had the highest groundwater elevation, but conversely also flushed a lot of salt into the groundwater, deteriorating the quality. The second highest groundwater elevation was observed in soil amendment, followed by control test cell. In terms of salinity, the soil amendment leached the least amount of TDS into the groundwater, followed by the control test cell. Moreover, infiltration rates in the native soil increased under longer detention times.

One of the major implications of the study is that detention basins retrofitted with trench aggregates and soil amendment can help promote recharge throughout the year and are applicable in regions that are prone to higher land subsidence. When the groundwater quality is of utmost concern, soil amendment is advantageous. Another important outcome of this study was that detention basins are not only beneficial to store water during major storm events, but they can also promote groundwater recharge without any further treatment when stormwater is detained for longer durations, provided the surface soils in the area possess high infiltration capacity (e.g., sandy loam) and the underlying subsurface geology is characterized by high horizontal hydraulic conductivity to facilitate lateral groundwater flow. Since detention basins in Harris County are designed to store water for no more than 24 hours (then the water is released back into the stream), longer detention times could be achieved by modifying outlet structures. A major concern associated with native soil is that it flushes a lot of salt during infiltration which renders the groundwater unusable for drinking purposes. This problem can be addressed by

636 treatments such as reverse osmosis. On the other hand, the groundwater derived from soil
637 amendment has lower concentration of total dissolved solids in it, so retrofitting the detention
638 basins with soil amendment would have a dual purpose in augmenting recharge and the reduction
639 of the salinity of recharged water.

640 Although this study was successfully able to establish that both LID systems and native soil
641 composed of sandy loam or similar texture can help enhance groundwater recharge, it was
642 beyond the scope of the study to compare the groundwater mounding and its extent under the test
643 cells for extreme rainfall events. Future research could include numerical modeling to evaluate
644 the stretch of groundwater mounding under different precipitation scenarios and more so for
645 other soil types or geologic frameworks. Investigating groundwater mounding would help
646 ascertain the desirable depth to the seasonally high water table which would improve the
647 performance of the LID practice. Another limitation of this study relates to its scalability, as the
648 test cells are relatively small (30.5 m x 30.5 m). Larger scale implementations may encounter
649 more soil heterogeneity and significant development of preferential flow paths, which could
650 influence the drainage patters and alter the groundwater recharge rates.

651 This study provides potential ways to address groundwater decline experienced in many parts of
652 the world by applying MAR using LID practices. This work also assessed the groundwater
653 recharge potential under ponding conditions. The results obtained from this research can be used
654 to effectively design new detention basins in areas with similar hydrogeology to not only store
655 stormwater during flood events but also promote groundwater recharge. Stormwater ponds
656 already in place could be retrofitted with LID systems such that excess rainfall runoff can be
657 used to replenish groundwater resources while lowering the hazards of excessive groundwater
658 consumption.

ACKNOWLEDGEMENTS

This project was funded by Harris County Flood Control District, Harris County Precinct 4, and Binkley & Barfield Inc. The authors appreciate the following collaborators and students for their help in the field work: Zhuping Sheng, Ph.D., P.E., P.H., Steven F. Albert, P.E., Christian Mosley, Ryan Edwards, Jorge S. Ramirez, Emily Schweizerhof, Janci McClellan, Jose Sagrera, Anshul Yadav, and Jaeyoung Song. The authors are especially grateful to Steven F. Albert, P.E., for his insights and critique on the study. The authors would also like to thank Ryan Edwards for his help with data processing, Jorge S. Ramirez for his help with figure preparation, and Emily Schweizerhof for her feedback on the manuscript.

AUTHOR'S NOTE

The authors do not have any conflicts of interest or financial disclosures to report.

DATA AVAILABILITY STATEMENT

Data will be made available on request.

REFERENCES

Ackerman, D., and E. D. Stein. 2008. "Evaluating the effectiveness of best management practices using dynamic modeling." *Journal of Environmental Engineering*, 134, 628–639. https://doi.org/10.1061/(ASCE)0733-9372(2008)134:8(628)

Ahiablame, L.M., B.A. Engel, and I. Chaubey. 2012. “Effectiveness of low impact development practices: literature review and suggestions for future research.” *Water, Air, & Soil Pollution,* 223, 4253–4273. https://doi.org/10.1007/s11270-012-1189-2

Ahiablame, L. M., B. A. Engel, and I. Chaubey. 2013. "Effectiveness of low impact development practices in two urbanized watersheds: Retrofitting with rain barrel/cistern and porous pavement." *Journal of Environmental Management*, *119*, 151–161. https://doi.org/10.1016/j.jenvman.2013.01.019

Associated Press. 2017. “Why Does Houston Flood So Often and So Heavily?” *NBC News*, 27 Aug. 2017. https://www.nbcnews.com/storyline/hurricane-harvey/why-does-houston-flood-so-often-so-heavily-n796446/

ASTM. 2018. “Standard Test Method for Infiltration Rate of Soils in Field Using Double-Ring Infiltrometer.” (ASTM Method D3385-18). https://www.astm.org/d3385-18.html

ASTM. 2017. “Standard Test Methods for Particle-Size Distribution (Gradation) of Soils Using Sieve Analysis.” (ASTM Method D6913-04). https://www.astm.org/standards/d6913

ASTM. 2017. “Standard Test Method for Particle-Size Distribution (Gradation) of Fine-Grained Soils Using the Sedimentation (Hydrometer) Analysis.” (ASTM Method D7928). https://www.astm.org/d7928-21e01.html

Aviles Engineering Corporation. 2003. “Geotechnical investigation for mitigation basin M525-01-00 and detention basin M525-02-00”. Reported to *Harris County Flood Control District, Houston, Texas*.

Baker, E.T. Jr. 1979. “Stratigraphic and hydrogeologic framework of part of the coastal plain of Texas.” *Texas Department of Water Resources*, Report 236, 43. https://pubs.usgs.gov/of/1977/0712/report.pdf

Bhaskar, A. S., D. M. Hogan, J. R. Nimmo, and K. S. Perkins. 2018. "Groundwater recharge amidst focused stormwater infiltration." *Hydrological Processes*, *32*(13), 2058–2068. https://doi.org/10.1002/hyp.13137

Blackburn, J., and J. Borski. 2023. “Assessing Houston’s Flood Vulnerability 6 Years After Harvey.” *Houston: Rice University’s Baker Institute for Public Policy*. Assessing Houston’s Flood Vulnerability 6 Years After Harvey | Baker Institute

Bouwer, H. 2002. “Artificial recharge of groundwater: hydrogeology and engineering”. *Hydrogeology Journal,* 10, 121-142. https://doi.org/10.1007/s10040-001-0182-4

Brander, K.E., K.E. Owen, and K.W. Potter. 2004. “Modeled impacts of development type on runoff volume and infiltration performance.” *Journal of the American Water Resources Association,* 40(4), 961-969. https://doi.org/10.1111/j.1752-1688.2004.tb01059.x

Brown, R.R., N. Keath, and T.H.F. Wong. 2009. “Urban water management in cities: historical, current and future regimes.” *Water Science & Technology*, 59 (5), 847–855. https://doi.org/10.2166/wst.2009.029

Carleton, G.B. 2010. “Simulation of groundwater mounding beneath hypothetical stormwater infiltration basins.” *U.S. Geological Survey Scientific Investigations Report* 2010-5102, 64 p. https://pubs.usgs.gov/sir/2010/5102/

717 Chowdhury, A.H., and M.J. Turco. 2006. “Geology of the Gulf Coast Aquifer, Texas.” *Texas*
718 *Water Development Board*, 365, 23-50.
719 https://www.twdb.texas.gov/publications/reports/numbered_reports/doc/R365/ch02-Geology.pdf

720 Chui, T.F.M., and D.H. Trinh. 2016. “Modelling infiltration enhancement in a tropical urban
721 catchment for improved stormwater management.” *Hydrological Processes*, 30 (23),4405–4419.
722 https://doi.org/10.1002/hyp.10926

723 Construction EcoServices. 2019. “smartPOND® Automated Stormwater Control.”
724 https://www.constructionecoservices.com/products-bmps/permanent-bmps/batch-detention-
725 smart-ponds/

726 Credit Valley Conservation Authority, and Toronto Region Conservation Authority. 2010. “Low
727 Impact Development Stormwater Management Planning and Design Guide.” Version 1.0. A
728 Publication of CVCA and TRCA. http://www.creditvalleyca.ca/wp-
729 content/uploads/2014/04/LID-SWM-Guide-v1.0_2010_1_no-appendices.pdf

730 Damodaram, C., M.H. Giacomoni, C. Prakash Khedun, H. Holmes, A. Ryan, W. Saour, and
731 E.M. Zechman. 2010. “Simulation of combined best management practices and low impact
732 development for sustainable stormwater management.” *Journal of the American Water*
733 *Resources Association,* 46(5), 907-918. https://doi.org/10.1111/j.1752-1688.2010.00462.x

734 Darling, B. K. 2016. "Geochemical Factors Controlling the Mobilization of Arsenic at an
735 Artificial Recharge Site, Clearwater, Florida." Journal of Contemporary Water Research &
736 Education, 159(1), 105–116. https://doi.org/10.1111/j.1936-704X.2016.03232.x

737 de Lambert, J. R., J. F. Walsh, D. P. Scher, A. D. Firnstahl, and M. A. Borchardt. 2021.
738 "Microbial pathogens and contaminants of emerging concern in groundwater at an urban

subsurface stormwater infiltration site." Science of The Total Environment, 775, 145738. https://doi.org/10.1016/j.scitotenv.2021.145738

DEP. 2006. Pennsylvania stormwater best management practices manual. *Pennsylvania Department Of Environmental Protection, US.* https://www.stormwaterpa.org/bmp-manual-chapter-6.html

Eckart, K., Z. McPhee, and T. Bolisetti. 2017. "Performance and implementation of low impact development – A review." *Science of The Total Environment*, 607-608, 413-432. https://doi.org/10.1016/j.scitotenv.2017.06.254

Ellis, J. H., J. E. Knight, J. T. White, M. Sneed, J. D. Hughes, J. K. Ramage, C. L. Braun, A. Teeple, L. K. Foster, S. H. Rendon, and J. T. Brandt. 2023. "Hydrogeology, land-surface subsidence, and documentation of the Gulf Coast Land Subsidence and Groundwater-Flow (GULF) model, southeast Texas, 1897–2018." In Professional Paper (1877). U.S. Geological Survey. https://doi.org/10.3133/pp1877

EPA (U.S. Environmental Protection Agency). 2013. "Secondary Drinking Water Regulations: Guidance for Nuisance Chemicals." Washington DC: EPA Office of Water. https://www.epa.gov/sdwa/drinking-water-regulations-and-contaminants

Fiori, A., and E. Volpi. 2020. "On the Effectiveness of LID Infrastructures for the Attenuation of Urban Flooding at the Catchment Scale." Water Resources Research, 56(5), e2020WR027121. https://doi.org/10.1029/2020WR027121

Fischer, D., E. G. Charles, and A. L. Baehr. 2003. "Effects of Stormwater Infiltration on Quality of Groundwater Beneath Retention and Detention Basins." *Journal of Environmental Engineering*, 129 (5). https://doi.org/10.1061/(ASCE)0733-9372(2003)129:5(464)

761 Harris County Flood Control district and Harris County Public Infrastructure Department
762 Architecture & Engineering Division. 2011. “Harris County Low Impact Development & Green
763 Infrastructure Design Criteria for Storm Water Management”. https://texasriparian.org/wp-
764 content/uploads/2013/02/Harris-County-LID-and-GI-Design-Criteria-Manual.pdf

765 Ganot, Y., R. Holtzman, N. Weisbrod, I. Nitzan, Y. Katz, and D. Kurtzman. 2017. "Monitoring
766 and modeling infiltration–recharge dynamics of managed aquifer recharge with desalinated
767 seawater." Hydrology and Earth System Sciences, 21(9), 4479–4493.
768 https://doi.org/10.5194/hess-21-4479-2017

769 Greuter, A., and C. Petersen. 2021. "Determination Of Groundwater Withdrawal And
770 Subsidence in Harris and Galveston Counties – 2020." https://hgsubsidence.org/wp-
771 content/uploads/2021/05/2020-HGSD-AGR_Executive-Summary_Final.pdf

772 Harris County Flood Control District. 2021. Stream elevation sensor 1339 located at 1340
773 Willow Creek at SH-249. https://www.harriscountyfws.org/

774 Hillel, D. 1998. “Environmental Soil Physics: Fundamentals, Applications, and Environmental
775 Considerations.” *Academic Press*, Waltham.

776 Horst, M., A. L. Welker, and R. G. Traver. 2011. “Multiyear Performance of a Pervious
777 Concrete Infiltration Basin BMP.” *Journal of Irrigation and Drainage Engineering*, 137 (6).
778 https://doi.org/10.1061/(ASCE)IR.1943-4774.0000302

779 Hu, M., X. Zhang, Y. Li, H. Yang, and K. Tanaka. 2019. "Flood mitigation performance of low
780 impact development technologies under different storms for retrofitting an urbanized area."
781 Journal of Cleaner Production, 222, 373–380. https://doi.org/10.1016/j.jclepro.2019.03.044

Jackisch, N., and M. Weiler. 2017. "The hydrologic outcome of a Low Impact Development (LID) site including superposition with streamflow peaks." Urban Water Journal, 14(2), 143–159. https://doi.org/10.1080/1573062X.2015.1080735

Kasmarek, M.C., and J.L. Robinson. 2004. “Hydrogeology and simulation of ground-water flow and land-surface subsidence in the northern part of the Gulf Coast aquifer system, Texas.” *U.S. Geological Survey Scientific Investigations Report*, 5102, 111. https://pubs.usgs.gov/sir/2004/5102/pdf/sir2004-5102.pdf

Lebon, Y., C. François, S. Navel, F. Vallier, L. Guillard, L. Pinasseau, L. Oxarango, L. Volatier, and F. Mermillod-Blondin. 2023. "Aquifer recharge by stormwater infiltration basins: Hydrological and vadose zone characteristics control the impacts of basins on groundwater chemistry and microbiology." Science of The Total Environment, 865, 161115. https://doi.org/10.1016/j.scitotenv.2022.161115

Liu, T., Y. Lawluvy, Y. Shi, and P.-S. Yap. 2021. "Low Impact Development (LID) Practices: A Review on Recent Developments, Challenges and Prospects." Water, Air, & Soil Pollution, 232(9), 344. https://doi.org/10.1007/s11270-021-05262-5

Lopes Bezerra, P. H., A. P. Coutinho, L. Lassabatere, S. M. dos Santos Neto, T. dos A. T. de Melo, A. C. D. Antonino, R. Angulo-Jaramillo, and S. M. G. L. Montenegro. 2022. "Water Dynamics in an Infiltration Trench in an Urban Centre in Brazil: Monitoring and Modelling." Water, 14(4), Article 4. https://doi.org/10.3390/w14040513

Lu, P., Z. Sheng, Z. Zhang, G. Miller, S. Reinert, and M. Huang. 2021. “Effect of multilayered groundwater mounds on water dynamics beneath a recharge basin: Numerical simulation and assessment of surface injection.” *Hydrological Processes,* 35, 1-20. https://doi.org/10.1002/hyp.14193

Machusick, M., A. Welker, and R. Traver. 2011. “Groundwater Mounding at a Storm-Water Infiltration BMP.” *Journal of Irrigation and Drainage Engineering*, 137 (3). https://doi.org/10.1061/(ASCE)IR.1943-4774.0000184

Masetti, M., D. Pedretti, A. Sorichetta, S. Stevenazzi, and F. Bacci. 2016. "Impact of a Storm-Water Infiltration Basin on the Recharge Dynamics in a Highly Permeable Aquifer." Water Resources Management, 30(1), 149–165. https://doi.org/10.1007/s11269-015-1151-3

McGrane, S.J. 2016. “Impacts of urbanisation on hydrological and water quality dynamics, and urban water management: a review.” *Hydrological Sciences Journal*, 61(13). https://doi.org/10.1080/02626667.2015.1128084

McQuiggan, R., A. S. Andres, A. Roros, and N. C. Sturchio. 2022. "Stormwater drives seasonal geochemical processes beneath an infiltration basin." Journal of Environmental Quality, 51(6), 1198–1210. https://doi.org/10.1002/jeq2.20416

METER Group, Inc. 2018. ATMOS 41. METER Environment. http://library.metergroup.com/Manuals/20635_ATMOS41_Manual_Web.pdf

METER Group, Inc. 2018. CTD-10. METER Environment. https://library.metergroup.com/Manuals/20908_HYDROS21_GEN2_Manual_Web.pdf

METER Group, Inc. 2018. G3 Drain Gauge. METER Environment. https://library.metergroup.com/Manuals/20677_G3_Manual_Web.pdf

METER Group, Inc. 2018. Teros 11/12. METER Environment. http://publications.metergroup.com/Manuals/20587_TEROS11-12_Manual_Web.pdf

Meyer, W.R., and J.E. Carr. 1979. “A digital model for simulation of ground-water hydrology in the Houston area, Texas.” *Texas Department of Water Resources, United States Geological Survey*, http://www.twdb.texas.gov/publications/reports/limited_printing/doc/LP-103/LP-103%20a.pdf

Mooers, E.W., R. C. Jamieson, J. L. Hayward, J. Drage, and C. B. Lake. 2018. “Low-Impact Development Effects on Aquifer Recharge Using Coupled Surface and Groundwater Models.” *Journal of Hydrologic Engineering*, 23(9). https://doi.org/10.1061/(ASCE)HE.1943-5584.0001682

MPCA. 2013. Minnesota Stormwater Manual. *Minnesota Pollution Control Agency, US.* https://stormwater.pca.state.mn.us/index.php?title=MS4_fact_sheet_-_Volume_Control_Using_Compost_Materials_/_Soil_Amendments

Muñoz, L. A., F. Olivera, M. Giglio, and P. Berke. 2018. "The impact of urbanization on the streamflows and the 100-year floodplain extent of the Sims Bayou in Houston, Texas." International Journal of River Basin Management, 16(1), 61–69. https://doi.org/10.1080/15715124.2017.1372447

Newcomer, M. E., J. J. Gurdak, L. S. Sklar, and L. Nanus. 2014. “Urban recharge beneath low impact development and effects of climate variability and change.” *Water Resources Research*, 50(2), 1716-1734. https://doi.org/10.1002/2013WR014282

NIDIS. 2024. “Historical Drought Conditions of Harris County.” https://www.drought.gov/historical-information?dataset=0&selectedDateUSDM=20241224&state=Texas&countyFips=48201

Puls, R.W., and M.J. Barcelona. 1996. “Low-flow (minimal drawdown) ground-water sampling procedures.” *EPA Ground Water Issue*, EPA/540/S-95/504, USEPA, Washington, DC. https://www.epa.gov/remedytech/low-flow-minimal-drawdown-ground-water-sampling-procedures

Rentachintala, L. R. N. P., M. G. M. Reddy, and P. K. Mohapatra. 2022. "Urban stormwater management for sustainable and resilient measures and practices: A review." Water Science and Technology, 85(4), 1120–1140. https://doi.org/10.2166/wst.2022.017

Shafique, M., R. Kim, and K. Kyung-Ho. 2018. "Evaluating the Capability of Grass Swale for the Rainfall Runoff Reduction from an Urban Parking Lot, Seoul, Korea." International Journal of Environmental Research and Public Health, 15(3), Article 3. https://doi.org/10.3390/ijerph15030537

Smith, W. B., G. R. Miller, and Z. Sheng. 2017. “Assessing aquifer storage and recovery feasibility in the Gulf Coastal Plains of Texas.” *Journal of Hydrology: Regional Studies*. 14, 92–108. https://doi.org/10.1016/j.ejrh.2017.10.007

Texas Living Waters. 2017. "Subsidence in the Houston-Galveston region: A new tool to learn from the past." https://texaslivingwaters.org/houston-subsidence-mapping-tool/

USEPA. 2003. “Wastewater Technology Fact Sheet, Rapid Infiltration Land Treatment.” Fact Sheet EPA 832-F-03-025. *United States Environmental Protection Agency*. https://www3.epa.gov/npdes/pubs/final_rapidinfiltration.pdf.

USGS. 2023. "Texas Gulf Coast Groundwater and Land Subsidence—Over Forty Years of Research in the Houston-Galveston Region." https://txpub.usgs.gov/houston_subsidence/archive.min/viewer.html

868 Voisin, J., B. Cournoyer, A. Vienney, and F. Mermillod-Blondin. 2018. "Aquifer recharge with
869 stormwater runoff in urban areas: Influence of vadose zone thickness on nutrient and bacterial
870 transfers from the surface of infiltration basins to groundwater." Science of The Total
871 Environment, 637–638, 1496–1507. https://doi.org/10.1016/j.scitotenv.2018.05.094

872 Wang, M., D. Zhang, Y. Cheng, and S. K. Tan. 2019. "Assessing performance of porous
873 pavements and bioretention cells for stormwater management in response to probable climatic
874 changes." Journal of Environmental Management, 243, 157–167.
875 https://doi.org/10.1016/j.jenvman.2019.05.012

876 Wild, T. B., and A. P. Davis. 2009. “Simulation of the performance of a storm-water BMP.”
877 *Journal of Environmental Engineering*, 135(12), 1257–1267.
878 https://doi.org/10.1061/(ASCE)EE.1943-7870.0000106

879 Yihdego, Y. 2017. "Simulation of Groundwater Mounding Due to Irrigation Practice: Case of
880 Wastewater Reuse Engineering Design." Hydrology, 4(2), Article 2.
881 https://doi.org/10.3390/hydrology4020019

882 Zahmatkesh, Z., S.J. Burian, M. Karamouz, H. Tavakol-Davani, and E. Goharian. 2014. “Low-
883 impact development practices to mitigate climate change effects on urban stormwater runoff:
884 case study of New York City.” *Journal of Irrigation and Drainage Engineering,* 141(1).
885 https://doi.org/10.1061/(ASCE)IR.1943-4774.0000770

886 Zhang, K., and T. F. M. Chui. 2017. “Evaluating hydrologic performance of bioretention cells in
887 shallow groundwater.” *Hydrological Processes,* 31 (23): 4122–4135.
888 https://doi.org/10.1002/hyp.11308

889 Zhang, K., T. F. M. Chui, and Y. Yang. 2018. "Simulating the hydrological performance of low
890 impact development in shallow groundwater via a modified SWMM." Journal of Hydrology,
891 566, 313–331. https://doi.org/10.1016/j.jhydrol.2018.09.006

892 Zhang, K., and T. F. M. Chui. 2019. “A review on implementing infiltration-based green
893 infrastructure in shallow groundwater environments: Challenges, approaches, and progress.”
894 *Journal of Hydrology,* 579. https://doi.org/10.1016/j.jhydrol.2019.124089

895 Zhao, L., T. Zhang, J. Li, L. Zhang, and P. Feng. 2023. "Numerical simulation study of urban
896 hydrological effects under low impact development with a physical experimental basis." Journal
897 of Hydrology, 618, 129191. https://doi.org/10.1016/j.jhydrol.2023.129191